

Quantum resource degradation theory within the framework of observational entropy decomposition

Xiang Zhou^{1,2,*}

¹*School of Mathematics and Computational Science, Shangrao Normal College, Shangrao 334001, People's Republic of China*

²*Jiangxi Province Key Laboratory of Applied Optical Technology,*

School of Physical Science and Intelligent Education, Shangrao Normal University, Shangrao 334001, China

(Dated: December 17, 2025)

We introduce a theory of quantum resource degradation grounded in a decomposition of observational entropy, which partitions the total resource into inter-block coherence (\mathcal{C}_{rel}) and intra-block noise (\mathcal{D}_{rel}). Under free operations, the total quantum resource is transformed into classical noise while its overall quantity remains conserved. We demonstrate that the metric η functions as a diagnostic indicator, providing a new lens on optimization stagnation, particularly the barren plateau phenomenon in variational quantum algorithms. We substantiate this framework through rigorous mathematical analysis and numerical simulations, and we explore how these channels can be physically implemented in real quantum systems. Our approach offers a unified viewpoint on quantum thermalization, measurement-induced disturbance, and the degradation of quantum advantage in practical devices, while also improving optimization strategies for current and near-term noisy quantum hardware.

I. INTRODUCTION

Quantum technologies hold the potential for transformative progress by exploiting quantum resources such as coherence and entanglement. Quantum resource theory offers a rigorous mathematical framework to quantify these resources by distinguishing resource states from free states[1–6]. A foundational concept in this framework is monotonicity: resource measures must not increase under free operations. While this principle reliably describes the loss of resources, it also exposes a fundamental shortcoming: it does not reflect how the quality of those resources evolves.

This shortcoming has practical implications. In noisy quantum devices, algorithms frequently fail because coherence is effectively washed out by noise, yet conventional resource measures do not exhibit a corresponding sharp decline. This creates a paradox: we can quantify the amount of resource present, but not evaluate its quality. A quantum state may retain the same nominal resource budget even as its usefulness gradually deteriorates, analogous to a currency that keeps its face value while its real purchasing power plummets.

We address this paradox by formulating a theory of quantum resource degradation grounded in a decomposition of observational entropy (OE). OE measures the uncertainty of a quantum state with respect to a specified coarse-grained measurement scheme[7–14]. We demonstrate that this entropy can be structurally separated into two physically distinct components: inter-block coherence \mathcal{C}_{rel} (a valuable quantum resource) and intra-block fluctuations \mathcal{D}_{rel} (effectively classical noise). This decomposition reveals a generic degradation process: under free operations, \mathcal{C}_{rel} is transformed into \mathcal{D}_{rel} , while their sum $\mathcal{O}_{\mathcal{C}}$ stays approximately invariant. In this way, quantum coherence is irreversibly converted into classical noise, maintaining the overall uncertainty but degrading its quantum nature.

This finding carries far-reaching consequences for quantum physics. It explains why quantum algorithms can stagnate even when they have ample resources available, why noisy hardware may deliver poor performance despite maintaining low error rates, and how quantum advantage can fade gradually through subtle deterioration of state quality rather than a sudden depletion of resources. The core mechanism is precisely characterized: we establish a one-to-one mapping in which every unit of lost coherence is translated into exactly one unit of additional noise.

We put this theory to the test by examining a key unresolved problem in quantum computation: the barren plateau phenomenon (BPP) in variational quantum algorithms (VQAs)[15, 16]. While earlier accounts have focused on entanglement or randomness, we instead pinpoint the loss of resource quality as the fundamental driver. Our resource-purity measure η serves as an early-warning signal, forecasting when optimization is likely to fail before it actually does. By tracking η during the algorithm's execution, one can observe resource degradation in real time and take corrective measures before the variational optimization grinds to a halt.

Our work extends beyond quantum information science by introducing a unified framework for describing how quantum coherence deteriorates into classical noise—a process central to quantum measurement, thermalization, and the emergence of classical behavior from quantum systems. This quality-aware viewpoint not only identifies failure modes in quantum algorithms but also uncovers fundamental bounds on quantum phenomena in both natural and engineered settings.

The structure of the paper is as follows. Section II reviews OE and block coherence. Section III, we present our decomposition framework together with the corresponding degradation mechanism. Section IV contrasts our approach with existing methods. Section V applies the framework to the analysis of barren plateaus in variational quantum algorithms. Finally, Section VI explores broader implications and outlines possible directions for future work.

* zhoux2032@163.com

II. BACKGROUND KNOWLEDGE

This section reviews the essential background needed to follow the theory developed in this work.

A. Observational Entropy

For a coarse-graining $\mathcal{C} = \{\hat{P}_x\}$ and an initial state ρ , the OE is defined as[7]

$$S_{\mathcal{C}}(\rho) = - \sum_x p_x \log_2 \frac{p_x}{V_x}, \quad (1)$$

where $p_x = \text{Tr}[\hat{P}_x \rho \hat{P}_x]$ and $V_x = \text{Tr}[\hat{P}_x]$.

Following Refs. [12–14], we define

$$\mathcal{O}_{\mathcal{C}}(\rho) = S_{\mathcal{C}}(\rho) - S(\rho), \quad (2)$$

where $S(\rho) = -\text{Tr}(\rho \log_2 \rho)$ is the von Neumann entropy. This difference quantifies the state's quantum coherence (or superposition) relative to the chosen coarse-graining. It satisfies[12]:

(C1) $\mathcal{O}_{\mathcal{C}}(\rho) \geq 0$;

(C2) $\mathcal{O}_{\mathcal{C}}(\rho) = 0$ if and only if $\rho = \sum_x \frac{p_x}{V_x} \hat{P}_x$;

(C3) $\mathcal{O}_{\mathcal{C}}(U \rho U^\dagger) = \mathcal{O}_{\mathcal{C}}(\rho)$ for any unitary $U = \bigoplus_j U_j$ that commutes with the coarse-graining \mathcal{C} ;

(C4) $\mathcal{O}_{\mathcal{C}}(\rho)$ is convex in ρ .

These properties show that $\mathcal{O}_{\mathcal{C}}(\rho)$ behaves as a coarse-graining-dependent measure of quantum coherence that is meaningful across different physical settings, from many-body systems to few-level quantum platforms.

B. Resource theory of inter-block coherence

The resource theory of block coherence, originally proposed by Åberg[1], extends coherence theory from bases to general projective measurements. Let $\mathcal{H} = \bigoplus_x \mathcal{H}_x$ be a direct sum of orthogonal subspaces \mathcal{H}_x with corresponding projectors \hat{P}_x . The set of block-incoherent (BI) states is

$$\mathcal{I}_{\text{B}}(\mathcal{H}) = \left\{ \sum_x \hat{P}_x \sigma \hat{P}_x \mid \sigma \in \mathcal{S} \right\}. \quad (3)$$

The corresponding block-dephasing operation is

$$\Delta(\sigma) = \sum_x \hat{P}_x \sigma \hat{P}_x. \quad (4)$$

Maximally block-incoherent (MBI) operations Λ_{MBI} are quantum channels that map BI states to BI states[17–21]:

$$\Lambda_{\text{MBI}}[\mathcal{I}_{\text{B}}(\mathcal{H})] \subseteq \mathcal{I}_{\text{B}}(\mathcal{H}). \quad (5)$$

A standard measure of block coherence is the relative-entropy measure

$$\mathcal{C}_{\text{rel}}(\rho, \mathcal{C}) = S(\Delta[\rho]) - S(\rho). \quad (6)$$

It satisfies the following properties:

- **Faithfulness:** $\mathcal{C}_{\text{rel}}(\rho, \mathcal{C}) \geq 0$, with equality if and only if ρ is block-incoherent.
- **Monotonicity:** $\mathcal{C}_{\text{rel}}(\Lambda_{\text{MBI}}[\rho], \mathcal{C}) \leq \mathcal{C}_{\text{rel}}(\rho, \mathcal{C})$.
- **Convexity:** $\mathcal{C}_{\text{rel}}(\sum_x p_x \rho_x, \mathcal{C}) \leq \sum_x p_x \mathcal{C}_{\text{rel}}(\rho_x, \mathcal{C})$.

From a physical perspective, \mathcal{C}_{rel} quantifies the additional uncertainty associated with coherent superpositions between different blocks. Block dephasing removes this inter-block coherence, converting quantum superposition into classical mixtures and thereby increasing the von Neumann entropy.

III. QUANTUM RESOURCE DEGRADATION THEORY

Building on the notions of OE and block coherence introduced in Sec. II, we now present the decomposition framework that underpins our theory of quantum resource degradation.

A. OE Decomposition

For a coarse-graining \mathcal{C} and state ρ , we have the identity[11]

$$S_{\mathcal{C}}(\rho) = S \left[\sum_x \hat{P}_x \rho \hat{P}_x \right] + \sum_x p_x D[\rho_x \parallel \kappa_x]. \quad (7)$$

Here $\rho_x = \hat{P}_x \rho \hat{P}_x / p_x$ and $\kappa_x = \hat{P}_x / V_x$ is the maximally mixed state in block x . The quantity $D(\rho \parallel \sigma) = \text{Tr}[\rho(\log_2 \rho - \log_2 \sigma)]$ is the quantum relative entropy.

Using the definition $\mathcal{O}_{\mathcal{C}} = S_{\mathcal{C}} - S$, we obtain our central decomposition:

$$\mathcal{O}_{\mathcal{C}}(\rho) = \mathcal{C}_{\text{rel}}(\rho, \mathcal{C}) + \mathcal{D}_{\text{rel}}(\rho), \quad (8)$$

where $\mathcal{D}_{\text{rel}}(\rho) = \sum_x p_x D[\rho_x \parallel \kappa_x]$. In this work, we refer to $\mathcal{O}_{\mathcal{C}}(\rho)$ as the total inconsistency.

Equation (8) is a mathematical identity with clear physical content. The decomposition reflects a basic dichotomy in quantum dynamics: the inter-block coherence \mathcal{C}_{rel} quantifies quantum superposition between macroscopically distinct states, while the intra-block contribution \mathcal{D}_{rel} captures classical uncertainty within each macrostate. The conversion of \mathcal{C}_{rel} into \mathcal{D}_{rel} under free operations corresponds to the progressive loss of phase information, a mechanism central to quantum measurement and decoherence.

Within this framework, we identify a key degradation pathway in which quantum coherence is irreversibly converted into classical noise. This conversion can proceed while approximately conserving $\mathcal{O}_{\mathcal{C}}$, thereby explaining performance losses even when conventional resource measures remain nearly unchanged.

Although $\mathcal{O}_{\mathcal{C}}$ is not a standard coherence monotone in the usual resource-theoretic sense, it quantifies the total inconsistency between the quantum state and the classical reference frame specified by the coarse-graining. In this way it goes beyond conventional coherence measures, capturing both quantum and classical contributions to resource degradation.

This structural perspective addresses a fundamental limitation of standard resource theories: their inability to track changes in resource quality under free operations. It provides a physically transparent view of how quantum resources decay, with direct implications for settings such as VQAs, where the quality of the resource, rather than its bare quantity, ultimately sets the performance.

B. Resource Purity

Definition 1. (Resource Purity) For a coarse-graining $\mathcal{C} = \{\hat{P}_x\}$ and an initial state ρ , the purity of the resource is defined as

$$\eta(\rho) := \frac{\mathcal{C}_{\text{rel}}(\rho, \mathcal{C})}{\mathcal{O}_{\mathcal{C}}(\rho)}, \quad (9)$$

with the convention that $\eta(\rho) = 0$ when $\mathcal{O}_{\mathcal{C}}(\rho) = 0$, since in that case the state is fully consistent with the coarse-graining.

- **Physical meaning:** A large value of η (close to 1) indicates a high-quality resource, where the observed effect is mainly due to coherence rather than noise. A small value of η (close to 0) indicates that the apparent resource is largely contaminated by noise.
- **Example:** Suppose $\mathcal{O}_{\mathcal{C}} = 0.8$ with $\mathcal{C}_{\text{rel}} = 0.6$ and $\mathcal{D}_{\text{rel}} = 0.2$. Then $\eta = 0.75$. If, after some operation, η drops to 0.4, the resource quality has been significantly degraded.
- **Properties:** $0 \leq \eta \leq 1$. It is monotonic under free operations: $\eta(\Lambda(\rho)) \leq \eta(\rho)$ for any free operation Λ .

The definition of η is motivated by the one-way implication that if $\mathcal{O}_{\mathcal{C}}(\rho) = 0$, then $\mathcal{C}_{\text{rel}}(\rho, \mathcal{C}) = 0$, while the converse does not hold[12]. The ratio η quantifies what fraction of the observable effect $\mathcal{O}_{\mathcal{C}}$ is actually due to the useful resource. A larger value of η therefore signals a higher-quality resource state, whereas a smaller value indicates that the resource is overwhelmed by intra-block noise. In this way, η provides a quality-sensitive figure of merit for comparing resource states and for designing and optimizing distillation protocols across different physical platforms.

C. Nonconvexity of Total Inconsistency

The measure $\mathcal{O}_{\mathcal{C}}$, used throughout this work, is in general nonconvex. This raises a natural question: does nonconvexity undermine its status as a resource measure?

We argue the opposite: this nonconvexity reflects physical features that the standard resource-theoretic framework does not capture. The usual convexity requirement is based on the assumption that mixing states by free operations cannot create resources. By contrast, $\mathcal{O}_{\mathcal{C}}$ quantifies the mismatch between the system state ρ and a classical description specified by the coarse graining \mathcal{C} . This mismatch has two contributions: \mathcal{C}_{rel} (a standard resource) and \mathcal{D}_{rel} (a nonstandard one).

The nonconvexity of $\mathcal{O}_{\mathcal{C}}$ arises because mixing quantum states can increase the mismatch between the system state and the chosen classical reference, and this has direct physical implications:

- **Physical significance:** The nonconvexity encodes the basic quantum fact that coherent superpositions cannot be generated by classical mixing alone. An increase in $\mathcal{O}_{\mathcal{C}}$ under mixing signals the genuine creation of quantum resources from a classical perspective.
- **Compatibility with resource theory:** Although $\mathcal{O}_{\mathcal{C}}$ is nonconvex, the genuinely useful resource contribution, \mathcal{C}_{rel} , obeys all standard resource-theory axioms (faithfulness, monotonicity, convexity). In this way, our framework connects conventional convex resource theories with a more general description of quantum structure relative to classical coarse grainings.
- **Theoretical advantage:** The nonconvex character of $\mathcal{O}_{\mathcal{C}}$ allows it to track resource transformations that any convex measure necessarily overlooks. In particular, it captures degradation processes in which coherence is converted into classical noise without changing the total value of $\mathcal{O}_{\mathcal{C}}$.

This nonconvexity is therefore not a drawback, but a necessary feature that allows our framework to describe subtle degradation pathways in realistic quantum systems and to clarify how quantum coherence appears or disappears when viewed through a fixed classical coarse graining.

D. Degradation Channels

We aim to demonstrate how resource quality degrades via coherence-to-noise conversion, even when the total resource is only approximately conserved. To this end, we construct explicit degradation channels. We support this mechanism with rigorous mathematical proofs and numerical examples, and we discuss how such channels can be physically realized in experimentally relevant quantum systems.

The following definition characterizes the transformation of resources under free operations and provides the mathematical foundation for constructing degradation channels.

Definition 2. (Resource Transformation Pathway) Consider a coarse-graining $\mathcal{C} = \{\hat{P}_x\}$ and an initial state ρ . Under a free operation Λ , the resource transformation pathway is given by

$$\begin{aligned} \Delta\mathcal{C}_{\text{rel}} &= \mathcal{C}_{\text{rel}}(\Lambda(\rho), \mathcal{C}) - \mathcal{C}_{\text{rel}}(\rho, \mathcal{C}) \leq 0, \\ \Delta\mathcal{D}_{\text{rel}} &= \mathcal{D}_{\text{rel}}(\Lambda(\rho)) - \mathcal{D}_{\text{rel}}(\rho), \\ \Delta\mathcal{O}_{\mathcal{C}} &= \mathcal{O}_{\mathcal{C}}(\Lambda(\rho)) - \mathcal{O}_{\mathcal{C}}(\rho) = \Delta\mathcal{C}_{\text{rel}} + \Delta\mathcal{D}_{\text{rel}}, \end{aligned} \quad (10)$$

where $|\Delta\mathcal{C}_{\text{rel}}|$ quantifies the decrease in \mathcal{C}_{rel} , and $|\Delta\mathcal{D}_{\text{rel}}|$ quantifies the change in \mathcal{D}_{rel} .

In this work, we are particularly interested in regimes where, under a suitable class of free operations, coherence

is irreversibly converted into noise, that is, \mathcal{C}_{rel} decreases ($\Delta\mathcal{C}_{\text{rel}} < 0$) while \mathcal{D}_{rel} increases ($\Delta\mathcal{D}_{\text{rel}} > 0$).

Within this transformation pathway, we define degradation channels as free operations that systematically reduce the resource quality parameter η .

Definition 3. (Degradation channels) A degradation channel Λ is a free operation that systematically converts useful quantum coherence into classical noise, while approximately conserving the total amount of resource. We construct explicit examples of such degradation channels. A simple instance is

$$\Lambda_{\alpha,\beta}(\rho) = (1 - \alpha)\rho + \alpha\mathcal{D}_\beta(\rho), \quad (11)$$

where $\mathcal{D}_\beta(\rho) = \beta\Delta(\rho) + (1 - \beta)\sum_x \hat{P}_x |\psi_0\rangle\langle\psi_0| \hat{P}_x$. The parameter α controls the overall noise strength of the channel, while β tunes the relative weight of the two noise mechanisms, thus specifying the pathway by which quantum coherence is converted into classical noise.

- Why is this a free operation?

- $\Delta(\rho)$: The block-dephasing map Δ removes all inter-block coherences and is a standard free operation.
- $\sum_x \hat{P}_x |\psi_0\rangle\langle\psi_0| \hat{P}_x$: This map prepares a block-diagonal state by projecting the target ground state $|\psi_0\rangle$ into the different blocks. Such block-diagonal state preparation is free[17].
- $\mathcal{D}_\beta(\rho)$: This composite degradation map combines the two free noise mechanisms above with relative weight β .
- $\Lambda_{\alpha,\beta}(\rho)$: The channel $\Lambda_{\alpha,\beta}$ is a convex mixture of the identity channel, a dephasing map, and a block-projection map. Since the set of free states is convex and the constituent maps are free, $\Lambda_{\alpha,\beta}$ maps free states to free states and therefore qualifies as a free operation.
- **Physical and experimental role:** The channel $\Lambda_{\alpha,\beta}$ provides a controlled way to degrade quantum coherence into classical noise. It can be implemented to systematically probe how the resource monotone η evolves during VQA optimization and how different types of noise accumulate in realistic devices, thus connecting the abstract resource picture to experimentally relevant noise processes.

To rigorously clarify the mathematical properties and physical significance of η , we now state and prove the following proposition.

Proposition 1. The resource purity η satisfies the following properties:

1. **Boundedness:** For any state ρ , $0 \leq \eta(\rho) \leq 1$.
2. **Monotonicity under free operations:** For any free operation Λ (i.e., any MBI operation), $\eta(\Lambda(\rho)) \leq \eta(\rho)$.

3. **Strict decrease under degradation channels:** For any degradation channel $\Lambda_{\alpha,\beta}$ defined in Definition 3, with $\alpha > 0$ and $\beta \in [0, 1]$, if the initial state ρ satisfies $\mathcal{C}_{\text{rel}}(\rho, \mathcal{C}) > 0$, then $\eta(\Lambda_{\alpha,\beta}(\rho)) < \eta(\rho)$.

Proof: See Appendix VII.

The definition of degradation channels immediately implies the following corollary.

Corollary 1. Under Λ , the change in η is given approximately by

$$\eta(\Lambda(\rho)) \approx \eta(\rho) - \frac{|\Delta\mathcal{C}_{\text{rel}}|}{\mathcal{O}_{\mathcal{C}}(\rho)}, \quad (12)$$

where the ratio $\frac{|\Delta\mathcal{C}_{\text{rel}}|}{\mathcal{O}_{\mathcal{C}}(\rho)}$ quantifies the relative loss of coherence with respect to the total inconsistency.

If $\mathcal{O}_{\mathcal{C}}(\rho) = 0$, then $|\Delta\mathcal{C}_{\text{rel}}| = 0$ and $\eta(\rho) = 0$, and consequently $\eta(\Lambda(\rho)) = 0$. In this case the state carries no usable resource, and degradation channels cannot further reduce η . More generally, the value of η remains approximately invariant under degradation channels if and only if the change in $\mathcal{O}_{\mathcal{C}}$, $\Delta\mathcal{O}_{\mathcal{C}}$, is negligible.

Let $\Delta\eta = \eta(\rho) - \eta(\Lambda(\rho))$. The quantity $\Delta\eta$ characterizes how strongly the channel degrades the quality of the resource. We classify the severity of resource degradation into three levels according to the value of $\Delta\eta$:

- **Minor degradation** ($\Delta\eta \in (0, 0.2)$): The resource quality shows a slight decrease, which may result from weak noise or mild optimization stagnation.
- **Significant degradation** ($\Delta\eta \in [0.2, 0.4)$): The resource quality exhibits a clearly visible decline that can substantially affect the current quantum task, for example by degrading algorithmic performance.
- **Severe degradation** ($\Delta\eta \geq 0.4$): The resource quality undergoes a strong deterioration.

These thresholds for $\Delta\eta$ can be adjusted to accommodate systems of different sizes.

The following theorem, which constitutes the central result of our framework, reveals how resources are transformed under a suitable class of free operations.

Theorem 1. (Resource Degradation Mechanism) There exist a degradation channel Λ and quantum states ρ such that

1. Coherence decreases: $\Delta\mathcal{C}_{\text{rel}} < 0$.
2. Noise increases: $\Delta\mathcal{D}_{\text{rel}} > 0$.
3. Total resource is approximately conserved: $|\Delta\mathcal{D}_{\text{rel}}| \approx |\Delta\mathcal{C}_{\text{rel}}|$, so $\Delta\mathcal{O}_{\mathcal{C}} \approx 0$.

Under these conditions, the resource purity η decreases significantly ($\Delta\eta > 0$), demonstrating a marked loss of resource quality at essentially fixed total resource content.

Proof: See Appendix VIII. We provide an analytic example using a 4-dimensional system and a specific channel Λ_ε . For $\varepsilon = 0.26$, we obtain $\Delta\mathcal{C}_{\text{rel}} \approx -0.130$, $\Delta\mathcal{D}_{\text{rel}} \approx +0.129$, $\Delta\mathcal{O}_C \approx -0.001$, and $\Delta\eta \approx 0.287$, which confirms the mechanism.

This theorem captures the physical essence of degradation: even when the total amount of resource is effectively conserved, its usable quantum character deteriorates. In particular, coherence is irreversibly converted into classical noise, illustrating how quantum resources can lose operational value without changing their overall nominal quantity.

The evolution of the key physical quantities used in the proof of Theorem 1 (see Appendix VIII) is shown in Fig. 1. When ε approaches 1, the quantum state undergoes an almost complete collapse to $|00\rangle\langle 00|$. This extreme regime exhibits several features that lie outside the domain of interest for our theory.

Theorem 1 establishes the existence of degradation channels that implement the coherence-to-noise transformation. The proof does not rely on scanning the full parameter space. It suffices to demonstrate that such channels act as required within an appropriate parameter region. The essential degradation mechanism is already fully captured for $\varepsilon \in [0, 0.26]$, so extending the analysis to larger ε is not necessary to validate our theoretical claims. The observed conversion between coherence and noise in this interval provides direct evidence for the existence of the degradation channels described in Theorem 1. For clarity, we therefore restrict ε to the interval $[0, 0.5]$ in the main text.

Fig. 1(a) shows the evolution of the resource components as a function of ε . The quantity \mathcal{O}_C displays a convex dependence on ε in $[0, 0.26]$, while η decreases monotonically. The convex behavior of \mathcal{O}_C signals a non-monotonic degradation process: the resource does not decay linearly with the noise strength. The initial decrease corresponds to a temporary reduction in total inconsistency, while the subsequent recovery reflects compensating contributions from different resource components. Despite this variation, the value of \mathcal{O}_C at the end of the interval confirms the predicted approximate conservation of the total resource.

In contrast, η is strongly degraded throughout this region. The purity drops from approximately 0.58 to 0.29, a change of more than 0.2. According to the classification criteria introduced in this work, such a reduction in purity qualifies as a significant degradation. This illustrates that, within the physically relevant parameter range, coherence can be reliably converted into noise via the degradation channels of Theorem 1, while the total resource \mathcal{O}_C remains approximately conserved even as purity is substantially lost.

Fig. 1(b) shows the changes in the individual resource measures. \mathcal{C}_{rel} becomes negative, signaling decoherence. \mathcal{D}_{rel} becomes positive, signaling the generation of purity. \mathcal{O}_C stays close to zero in the degradation region, demonstrating that the total resource is conserved during the transformation.

Fig. 1(c) quantifies the conversion rate between \mathcal{C}_{rel} and \mathcal{D}_{rel} . The efficiency $\Delta\mathcal{D}_{\text{rel}}/|\mathcal{C}_{\text{rel}}|$ approaches unity in certain regions, indicating nearly ideal conversion: each unit of lost quantum coherence is converted into one unit of gained clas-

sical noise. This behavior confirms the theoretical prediction that, under optimal conditions, quantum coherence is converted directly into classical noise.

Fig. 1(d) tests the three conditions of Theorem 1 at the critical point, showing that $\Delta\mathcal{C}_{\text{rel}} < 0$, $\Delta\mathcal{D}_{\text{rel}} > 0$, and $\Delta\mathcal{O}_C \approx 0$ hold simultaneously. The pronounced drop in η indicates a degradation in resource quality, while the near-constancy of \mathcal{O}_C confirms that the total amount of resource is conserved.

E. Results and Discussion

Our framework offers a new diagnostic perspective on quantum optimization. In contrast to traditional explanations based mainly on entanglement saturation or randomness, our theory identifies resource-quality degradation as a fundamental mechanism behind optimization failure. The resource-purity metric η provides several distinct diagnostic capabilities:

Theoretical diagnostic framework:

Early-warning capability: A decrease in η typically precedes observable optimization stagnation, serving as an early indicator of resource-quality degradation.

Failure-mode discrimination: η distinguishes failures caused by insufficient resource quantity (low \mathcal{O}_C) from those caused by degraded resource quality (low η despite adequate \mathcal{O}_C).

Degradation-pathway identification: The conversion of coherence into noise ($\mathcal{C}_{\text{rel}} \rightarrow \mathcal{D}_{\text{rel}}$) provides a concrete microscopic pathway for performance deterioration.

In Sec. V we validate this framework by applying it to the barren-plateau problem in VQAs, and show that real-time monitoring of η can diagnose—and potentially help mitigate—optimization stagnation.

To highlight the conceptual innovations and distinctive features of the proposed theory, we now provide a systematic comparison with existing resource-theoretic approaches.

In this section, we position our framework within the broader landscape of quantum resource theories. By clarifying both the shared foundations and the distinctive features of our approach, we aim to highlight its theoretical novelty and practical relevance across subfields.

IV. COMPARISON WITH EXISTING RESOURCE THEORIES

This section places our theory within the broader landscape of quantum resource theories. By clarifying the common foundations and distinctive features of our approach, we aim to highlight its theoretical novelty and practical utility.

A. Contrast with Standard Scalar Resource Theories

Standard quantum resource theories provide a widely used framework for quantifying quantum advantage, built on the following elements:

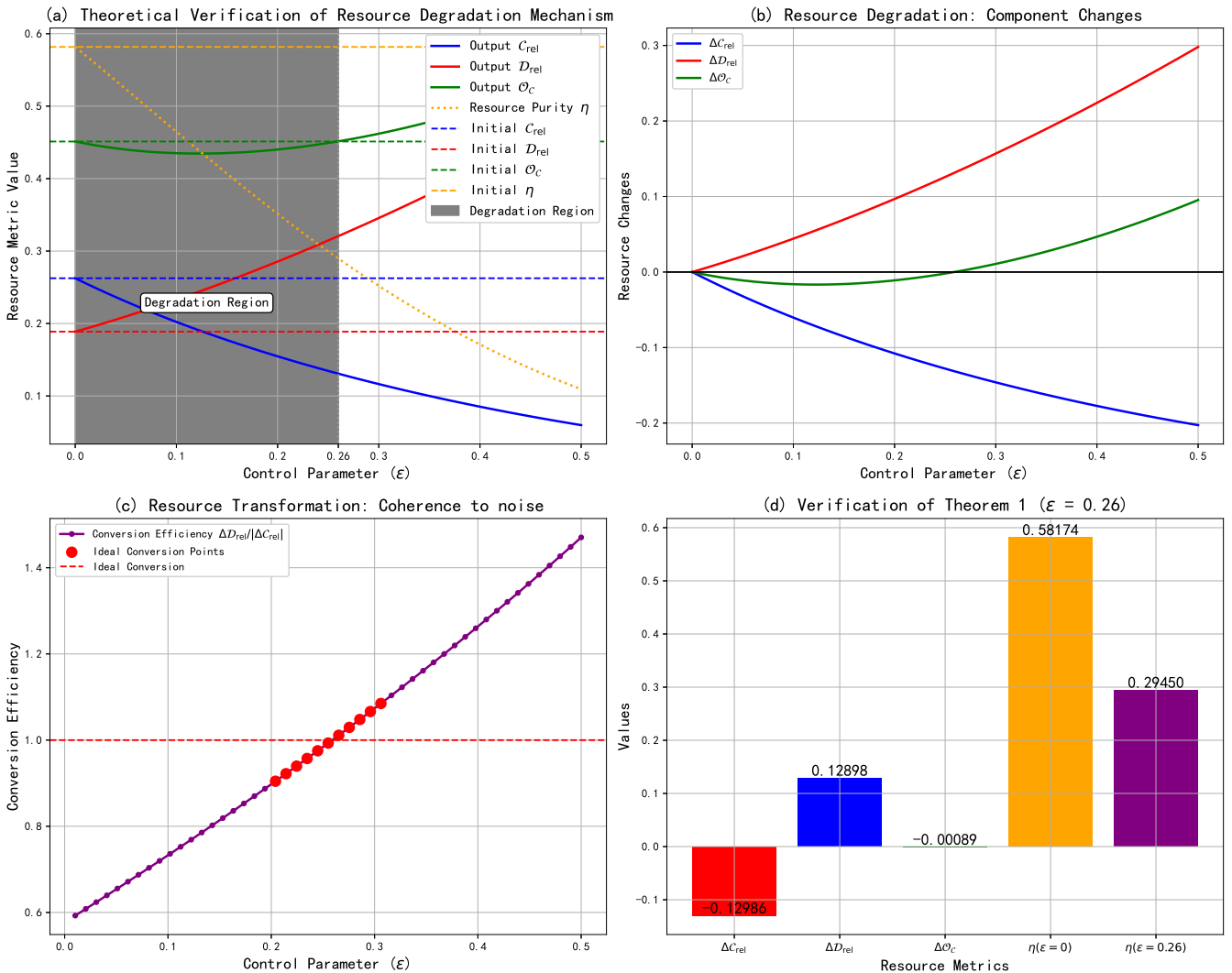


FIG. 1. In Fig. 1(a) and Fig. 1(b), the blue curves correspond to C_{rel} and ΔC_{rel} , the red curves correspond to D_{rel} and ΔD_{rel} , the green curves correspond to \mathcal{O}_C and $\Delta \mathcal{O}_C$, and the orange curve corresponds to η . Fig. 1(a) illustrates how the individual resource components change as ε is varied, whereas Fig. 1(b) displays the associated differential variations of the resource measures. Fig. 1(c) characterizes the conversion rate between C_{rel} and D_{rel} . Fig. 1(d) confirms that the three conditions of Theorem 1 hold at the critical point. The control parameter ε is tuned within the interval $[0, 0.5]$.

- **Free states (\mathcal{F}):** States that can be prepared at no cost under the relevant physical constraints.
- **Free operations (Λ_{free}):** Operations that cannot generate resource from free states.
- **Resource measures ($M(\rho)$):** Scalar functions that are monotonic under free operations, $M(\Lambda_{\text{free}}(\rho)) \leq M(\rho)$.

Our framework follows this general structure: the free states are block-incoherent (BI) states, the free operations include the degradation channels that we construct, and \mathcal{O}_C plays the role of a fundamental resource measure.

- **Free states:** BI states $\rho_{\text{BI}} = \sum_x \frac{p_x}{V_x} \hat{P}_x$.
- **Free operations:** Degradation channels Λ .

- **Resource measure:** Total inconsistency \mathcal{O}_C .

The conceptual contribution of our approach becomes most transparent when contrasted with standard scalar resource theories, as summarized in Table I.

Table I highlights a change of emphasis. Traditional resource theories monitor the degradation of a single total resource measure, $\Delta M \leq 0$. In contrast, our framework, built on the decomposition of OE, resolves the operational resource \mathcal{O}_C into two components, C_{rel} and D_{rel} , and tracks how they are converted into one another.

When $\Delta M \approx 0$, traditional approaches can only conclude that the total resource is essentially conserved, and therefore offer limited insight into why an algorithm deteriorates. Our framework instead captures situations in which performance worsens despite apparent resource conservation. The loss of performance is driven by the conversion of C_{rel} into D_{rel} ,

Aspect	Traditional Theory	Our Framework
Primary Focus	Total resource measure $M(\rho)$	Resource composition: \mathcal{C}_{rel} vs \mathcal{D}_{rel}
Resource Evolution	Degradation: $\Delta M \leq 0$	Conversion: $\mathcal{C}_{\text{rel}} \rightarrow \mathcal{D}_{\text{rel}}$
Diagnostic Power	Limited when $\Delta M \approx 0$	Reveals performance loss even when $\Delta \mathcal{O}_C \approx 0$
Quality Assessment	Not available	η quantifies resource quality
Barren Plateaus	Typically attributed to excessive entanglement or randomness	Attributed to degradation of resource quality

TABLE I. Comparison between a traditional resource-theoretic description and our framework.

which lowers η and thus degrades the quality of the resource rather than its total amount. This provides a physically transparent mechanism for performance degradation even when the total resource remains nearly unchanged.

This distinction is particularly relevant for phenomena such as barren plateaus, where the performance of VQAs collapses even though the underlying resource measure is conserved: in our picture, the plateau arises from a loss of resource quality, not from a loss of resource quantity.

B. Connection with Purity and Mixedness Measures

Conventional purity is typically quantified by the purity $\text{Tr}(\rho^2)$ or the von Neumann entropy $S(\rho) = -\text{Tr}(\rho \log_2 \rho)$. These are global measures characterizing a state's deviation from the maximally mixed state. Decoherence generally increases the mixedness of a system (equivalently, decreases its purity).

In our framework, \mathcal{D}_{rel} quantifies intra-block noise within coarse-grained subspaces, while η characterizes the quality of the resource. Our results show that, as a resource degrades, \mathcal{D}_{rel} increases whereas η decreases. At first sight, this seems to contradict the usual intuition that noise simply drives the system towards a more mixed state.

This apparent tension—that noise increases \mathcal{D}_{rel} while typically reducing global purity—is resolved by recognizing that the two quantities are defined with respect to different reference frames set by the coarse-graining. This distinction is summarized in Table II.

Aspect	Traditional Theory	Our Framework
Measure	Reference Frame	Physical Interpretation
$\text{Tr}(\rho^2)$	Full Hilbert space \mathcal{H}	Global mixedness
$\mathcal{D}_{\text{rel}}(\rho)$	Coarse-grained subspaces \mathcal{H}_x	Intra-block noise

TABLE II. Comparison between global purity $\text{Tr}(\rho^2)$ and intra-block noise $\mathcal{D}_{\text{rel}}(\rho)$, highlighting their distinct reference frames and physical meanings.

The resolution highlights the nuanced perspective of our framework. Free operations (such as block dephasing Δ) destroy \mathcal{C}_{rel} , making the state more mixed at the global level (i.e., increasing $S(\rho)$). However, within each coarse-grained subspace, such operations can drive the state toward a more deterministic distribution, thereby increasing its local predictability.

Consider a concrete physical scenario: a quantum state subject to dephasing noise:

- **Global perspective:** Coherence between blocks is destroyed \rightarrow increased mixedness \rightarrow reduced global purity.
- **Local perspective:** Within each block, the state can become more deterministic \rightarrow increased local predictability \rightarrow increased \mathcal{D}_{rel} .

Thus, \mathcal{D}_{rel} quantifies deviations from the maximally mixed state within each subspace. It captures a form of structured, intra-block noise, rather than featureless global randomness. In this sense, resource degradation corresponds to the conversion of useful nonlocal coherence into less useful intra-block noise.

C. Comparison with Traditional Entanglement Measures

The advantage of our metric η over traditional resource measures is illustrated by comparing it with entanglement entropy.

As shown in Table III, entanglement entropy is sensitive to the overall loss of resources but cannot distinguish between the conversion of coherence into noise and a simple reduction in the total amount of resources. In contrast, η is designed to detect resource quality degradation, providing a more refined diagnostic for optimization problems such as the barren plateau problem.

D. Summary of Theoretical Positioning

The above comparisons clarify the specific role of our framework. Rather than replacing existing resource theories, our approach integrates and extends them by introducing a structural perspective on how different forms of resources are composed and transformed. The central shift is from merely quantifying how much resource is present to characterizing *what form* that resource takes.

We achieve this by combining the notions of coherence and intra-block noise into a single global quantity, \mathcal{O}_C , and then analyzing the trade-off between its components under free operations. This unification enables our theory to

Aspect	Entanglement Entropy	Resource Purity η
Diagnostic role	Signals resource degradation	Quantifies resource quality degradation
Barren plateau insight	Identifies entanglement saturation	Reveals coherence-to-noise conversion
Response to noise	Typically decreases under decoherence	Selectively tracks quality loss
Guidance for optimization	Limited for assessing resource quality	Locates regions with high-quality resources

TABLE III. Comparison between entanglement entropy and the resource purity η , emphasizing their distinct diagnostic power for quantum resources across different platforms.

- Explain performance degradation in settings where traditional scalar measures predict resource conservation, thereby addressing a key limitation in current explanations of barren plateaus.
- Provide a quality-sensitive diagnostic (η) that yields early warnings and mechanistic insight beyond what can be inferred from entanglement measures or global mixedness alone.

In summary, this work establishes resource-quality management as a complementary paradigm to traditional resource quantification. It provides a more nuanced and broadly applicable framework for diagnosing and optimizing the performance of quantum technologies across different physical platforms and tasks.

V. RESOURCE DEGRADATION THEORY IN VQAS

The degradation mechanism we identify is not specific to VQAs. It is generic across quantum technologies. It appears in quantum sensing when phase sensitivity degrades even though the signal strength remains fixed, in quantum simulation when Trotter errors build up and act effectively as classical noise, and in quantum memories when the coherence time is limited not by leakage out of the code space but by scrambling within logical blocks.

We now apply our framework to VQAs. We show that the metric η serves as a diagnostic for optimization stagnation, in particular for the BPP. Using controlled numerical experiments, we track how the resource quality evolves during optimization, and we find that the observed behavior is consistent with the predictions of our degradation theory.

A. Experimental Setup

1. System Model and Hamiltonian

We study a four-qubit transverse-field Ising model with periodic boundary conditions, $Z_5 = Z_1$, described by the Hamiltonian[22]

$$H = - \sum_{i=1}^4 Z_i Z_{i+1} - h \sum_{i=1}^4 X_i. \quad (13)$$

We set the transverse field strength to $h = 1$, which corresponds to the quantum critical point of this model. We choose this system because it has a simple, well-resolved spectrum and well-characterized entanglement structure, providing a physically transparent basis for our coarse-graining scheme and making the results easily interpretable across subfields.

2. Coarse-Graining Scheme

In VQAs the objective is to prepare low-energy states of a target Hamiltonian. It is therefore natural to define the coarse graining in the energy eigenbasis. We introduce projectors

$$\hat{P}_x = \sum_{i \in I_x} |E_i\rangle\langle E_i|, \quad (14)$$

where I_x denotes the set of eigenstates in energy sector x , with $x \in \{\text{low, medium, high}\}$.

The Hilbert space is partitioned into three energy windows:

- **Low-energy subspace:** $E < E_{\min} + 0.3\Delta E$, where $\Delta E = E_{\max} - E_{\min}$.
- **Medium-energy subspace:** $E_{\min} + 0.3\Delta E \leq E \leq E_{\max} - 0.3\Delta E$.
- **High-energy subspace:** $E > E_{\max} - 0.3\Delta E$.

This coarse-grained energy resolution captures how the variational state migrates across the spectrum during optimization, allowing us to quantify resource degradation in a way that is directly tied to physically meaningful energy scales.

3. Cost Function

In this subsection, we define the cost function used to optimize the VQAs. The cost function is the expectation value of the system Hamiltonian with respect to the parameterized quantum state,

$$f(\vec{\theta}) = \langle \psi(\vec{\theta}) | H | \psi(\vec{\theta}) \rangle, \quad (15)$$

where $|\psi(\vec{\theta})\rangle$ is the ansatz state prepared by the parameterized quantum circuit $U(\vec{\theta})$, and $\vec{\theta}$ denotes the set of tunable circuit parameters.

4. Circuit Structure

We employ a hardware-efficient ansatz[23, 24], whose detailed architecture is shown in Fig. 4:

$$U(\vec{\theta}) = \left(\prod_{l=1}^4 \mathcal{L}_l(\vec{\theta}) \right) \left(\prod_{i=0}^3 H_i \right), \quad (16)$$

where

$$\mathcal{L}_l(\vec{\theta}) = \left(\prod_{i=0}^3 R_x(\vec{\theta}_{l,i}^x) R_y(\vec{\theta}_{l,i}^y) \right) \left(\prod_{i=0}^3 C X_{i,i+1} \right) \quad (17)$$

represents the l th circuit layer.

The circuit prepares the ansatz state $|\psi(\vec{\theta})\rangle$ by first applying a layer of Hadamard gates to all qubits, followed by $L = 4$ identical layers. Each layer $\mathcal{L}_l(\vec{\theta})$ consists of parameterized single-qubit rotations and a linear chain of CNOT gates that generate entanglement. With a total of 32 tunable parameters, this hardware-efficient design balances expressiveness against implementability on current and near-term noisy quantum devices. Its structure is particularly suited for systematically studying how resource degradation impacts variational performance.

5. Optimization Protocol and Parameter Update Rules

In this subsection, we describe the three-phase degradation protocol and the parameter update rule used during the optimization. This protocol mimics the evolution from an ideal optimization environment to one with strong degradation.

The degradation protocol specifies how artificially introduced noise changes over time, thereby emulating the accumulation of noise in realistic hardware that limits VQA performance.

It controls the strength of the degradation channel $\Lambda_{\alpha,\beta}$ [Eq. (11)] applied to the quantum state via the degradation parameter α . This channel systematically consumes the useful resource \mathcal{C}_{rel} and converts it into \mathcal{D}_{rel} , thereby directly reducing the efficiency η with which the VQA exploits its quantum resources across different noise regimes.

• Degradation Protocol:

- **Phase I (0–30):** No degradation ($\alpha = 0$). This phase represents an ideal, noiseless optimization environment, where the algorithm can fully explore the Hilbert space to locate the optimal solution. It provides a performance baseline under ideal conditions.
- **Phase II (30–60):** Linear ramp-up of degradation (α from 0.1 to 0.4). This phase mimics the onset of mild to moderate noise that begins to hinder the optimization process, analogous to running a medium-depth circuit on current or near-term noisy quantum devices. Here, we track how

an initial reduction in η slows down the optimization (for example, by reducing the descent rate of the cost function).

- **Phase III (60–150):** Strong degradation (α from 0.4 to 0.8). This phase corresponds to the algorithm operating in a regime of severe resource degradation, where noise dominates and destroys the quantum coherence required for useful computation. It illustrates that, even though the optimization formally continues (parameters are still updated), the cost function cannot improve further because of the poor resource quality; in other words, the algorithm enters a barren plateau induced by resource degradation.

The parameter-update rule specifies how the classical optimizer adjusts the circuit parameters $\vec{\theta}$ as a function of the current iteration and the associated cost. It is chosen to exhibit qualitatively distinct behavior in the different degradation phases, thereby modeling the optimizer’s response to varying noise levels.

• Parameter-update rule:

$$\vec{\theta}^{(k+1)} = \vec{\theta}^{(k)} + \Delta\vec{\theta}^{(k)} \pmod{2\pi}. \quad (18)$$

- $\Delta\vec{\theta}^{(k)}$ is the parameter update at iteration k , and its form depends on the degradation phase.

- * The index k labels the iteration step and serves as the temporal variable for the entire process. It marks the boundaries between degradation phases and underlies the definition of the progress variable p .
- * The variable p is a dimensionless progress parameter, defined as $p = (k - 30)/30$ in the mild-degradation phase and $p = (k - 60)/90$ in the strong-degradation phase.

• Early phase ($k \leq 30$):

$$\Delta\vec{\theta}^{(k)} = -0.05(0.1 \sin \vec{\theta}^{(k)} + \mathcal{N}(0, 0.05)). \quad (19)$$

In this effectively noiseless regime, the update uses a fixed learning rate of 0.05. The update combines a weak gradient-like signal, $0.1 \sin \vec{\theta}^{(k)}$, with a small stochastic exploration term, $\mathcal{N}(0, 0.05)$. This models efficient optimization in an ideal, low-noise setting.

- The symbol $\mathcal{N}(\mu, \sigma)$ denotes a random variable drawn from a Gaussian (normal) distribution with mean μ and standard deviation σ , representing stochastic fluctuations in the optimization process. In the early and mid phases, this noise facilitates exploration and helps the algorithm avoid shallow local minima. In the strong-degradation phase, it models optimization steps that become essentially random once the gradient signal is suppressed by resource degradation.

- **Mid phase** ($30 \leq k \leq 60$):

$$\begin{aligned}\Delta\vec{\theta}^{(k)} = & -0.03 \sin\vec{\theta}^{(k)} (1 - 0.5p) \\ & + 0.2p\mathcal{N}(0, 0.5).\end{aligned}\quad (20)$$

As the noise level α increases, the learning rate is reduced (from 0.05 to 0.03). The weight of the gradient term decreases (governed by the progress factor p), while the amplitude of the random noise increases significantly. This simulates the optimizer struggling and relying more on randomness for direction.

- **Strong degradation phase** ($k \geq 60$):

$$\begin{aligned}\Delta\vec{\theta}^{(k)} = & -0.01 \sin\vec{\theta}^{(k)} (0.5 - 0.4p) \\ & + 0.5\mathcal{N}(0, 1.0).\end{aligned}\quad (21)$$

Under strong noise, the learning rate is minimal (0.01). The weight of the gradient term decreases from 0.5 to 0.1 as p increases, becoming almost negligible. Concurrently, the random noise term $\mathcal{N}(0, 1.0)$ has a large amplitude and a high weight (0.5). Thus, the parameter updates become almost entirely random once the gradient signal vanishes—a hallmark of the BPP.

In summary, the degradation protocol and parameter update rule are intrinsically coupled. The protocol systematically reduces resource quality by tuning α , while the update rule captures the optimizer's response to this controlled degradation. As η decreases, the effective gradient signal available to the optimizer diminishes, and its dynamics cross over from directed gradient descent to essentially undirected random walks.

This controlled setting shows that a reduction in η precedes and drives the onset of optimization stagnation. In this way, the protocol provides a quantitative diagnostic for the BPP, clarifying how resource degradation translates into a loss of effective optimization dynamics that is relevant across optimization and learning problems in physics and beyond.

B. Resource evolution under degradation: theoretical and experimental analysis

This section analyzes the evolution of quantum resource metrics under degradation channels, building on the experimental framework in Sec. V A. We track the dynamics of the resource purity η and its components \mathcal{C}_{rel} and \mathcal{D}_{rel} to demonstrate that the loss of resource quality underlies the stagnation of VQA optimization.

Fig. 2 presents an experimental validation of quantum resource degradation through four complementary analyses.

Fig. 2(e) shows the progressive decline of the cost function under the three-phase degradation protocol. During Phase I (iterations 0–30), optimization proceeds efficiently in the absence of degradation. As degradation is introduced and increased in Phase II (30–60), optimization slows markedly.

In Phase III (60–150), the cost function becomes effectively frozen despite continued parameter updates, indicating that the degradation of resource quality drives the onset of barren-plateau-like behavior and halts further optimization progress.

Fig. 2(f) illustrates the underlying transformation mechanism through the evolution of the resource metrics. Out-of-phase oscillations between \mathcal{C}_{rel} and \mathcal{D}_{rel} reveal a systematic conversion of quantum coherence into classical noise. During this evolution, $\mathcal{O}_{\mathcal{C}}$ remains approximately conserved, indicating a redistribution of resources rather than a net loss. The monotonic decrease of η directly quantifies the gradual degradation of resource quality.

Fig. 2(g) focuses on the strong degradation regime (iterations 60–150), where the coherence-to-noise conversion is most pronounced. The persistent anticorrelation between \mathcal{C}_{rel} and \mathcal{D}_{rel} confirms the robustness of the conversion dynamics. Instances with $\Delta\mathcal{O}_{\mathcal{C}} \approx 0$ provide experimental support for Theorem 1, demonstrating a quantitative balance between loss of quantum coherence and generation of classical noise under conservation of the total resource.

Fig. 2(h) provides statistical support for this picture via a Pearson-correlation analysis.

The Pearson correlation coefficient r quantifies the linear relationship between two variables and is defined as

$$r = \frac{\sum_{i=1}^n (x_i - \bar{x})(y_i - \bar{y})}{\sqrt{\sum_{i=1}^n (x_i - \bar{x})^2 \sum_{i=1}^n (y_i - \bar{y})^2}}, \quad (22)$$

where x_i and y_i denote \mathcal{C}_{rel} and \mathcal{D}_{rel} at iteration i , respectively, and \bar{x} and \bar{y} are the corresponding sample means. The sample size is n (here, iterations 31–149).

The Pearson correlation coefficient r and the p -value in Fig. 2(h) demonstrate a statistically significant inverse relationship. The coefficient $r = -0.9309$ quantifies the strong negative linear correlation between \mathcal{C}_{rel} and \mathcal{D}_{rel} , while the p -value ($p \approx 0$) indicates extremely high statistical significance. This p -value represents the probability of observing such a strong correlation by random chance under the null hypothesis of no relationship. The combination of r approaching -1 and $p < 0.001$ provides compelling evidence against the null hypothesis, confirming that the observed anti-correlation is genuine and not due to random fluctuations. This statistical relationship supports the theoretical prediction of systematic conversion between coherence and noise components during resource degradation.

We determine the confidence interval for r using the Fisher Z transformation, a standard method for correlation coefficients.

First, apply the Fisher Z transformation:

$$Z = \frac{1}{2} \log_2 \left(\frac{1+r}{1-r} \right). \quad (23)$$

The standard error of Z is

$$SE_Z = \frac{1}{\sqrt{n-3}}. \quad (24)$$

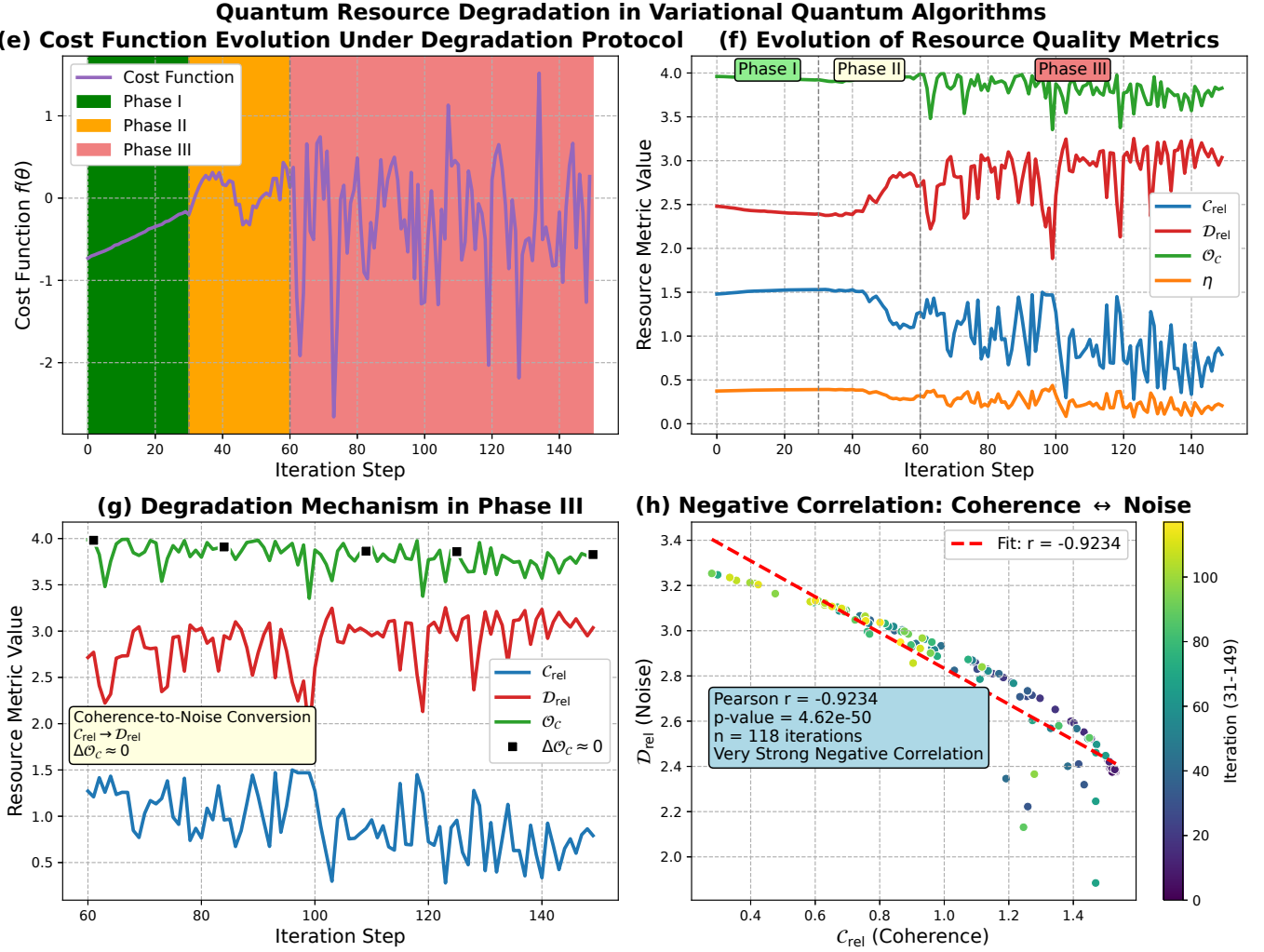


FIG. 2. Verification of quantum resource degradation in VQAs. Fig. 2(e) shows the evolution of the cost function, while Fig. 2(f) and Fig. 2(g) show the dynamics of the resource metrics for $\beta = 0.74$, and Fig. 2(h) shows the Pearson correlation between C_{rel} and D_{rel} .

For a 95% confidence interval, the bounds in the Z domain are

$$Z_{\text{lower}} = Z - 1.96 \times SE_Z, \quad (25)$$

$$Z_{\text{upper}} = Z + 1.96 \times SE_Z. \quad (26)$$

Finally, we transform these bounds back to the correlation domain. For a given Z we have

$$r = \frac{e^{2Z} - 1}{e^{2Z} + 1}, \quad (27)$$

which is applied to Z_{lower} and Z_{upper} to obtain the confidence interval for r .

This statistical characterization of the correlation between C_{rel} and D_{rel} provides a quantitative measure of how tightly these quantum quantities co-vary across iterations, in a form that is directly comparable to correlation analyses used throughout many areas of physics.

To further verify the statistical reliability of the negative correlation between C_{rel} and D_{rel} , we have performed

20 independent repetitions of the experiment under identical initial conditions (see Table IV and Fig. 3). The Pearson correlation coefficients obtained from these runs have a mean value of -0.8999 with a standard deviation of 0.0446 . The 95% confidence interval for the mean correlation coefficient is $[-0.9293, -0.8590]$, which is well separated from zero, providing strong evidence against the null hypothesis of no correlation. All runs yielded p -values less than 0.001 , confirming the statistical significance of the observed anti-correlation. This consistency across multiple independent realizations demonstrates the robustness of the coherence-to-noise conversion mechanism that governs resource degradation in VQAs.

The consistent negative correlation observed across all experiments (mean $r = -0.8999$, 95% CI $[-0.9293, -0.8590]$) confirms the robustness of the coherence-to-noise transformation mechanism. The narrow confidence interval and small standard deviation (0.0446) indicate high reproducibility of the results. The interquartile range of 0.0643 demonstrates moderate variability in the correlation coefficients across ex-

TABLE IV. Statistical summary of 20 independent runs with $\beta = 0.74$.

Statistic	Value	Interpretation
Number of experiments	20	Independent runs with different random seeds
Mean Pearson r	-0.8999	Average correlation coefficient
Standard deviation of r	0.0446	Spread of correlation coefficients across runs
95% CI lower bound	-0.9293	Lower limit of the 95% confidence interval
95% CI upper bound	-0.8590	Upper limit of the 95% confidence interval
Mean p -value	3.75e-30	Average significance level (all $p < 10^{-3}$)
t -statistic (vs. zero)	-87.8932	Test statistic for $H_0: \text{mean}(r) = 0$
p -value of t -test	2.89e-26	p -value under the null hypothesis

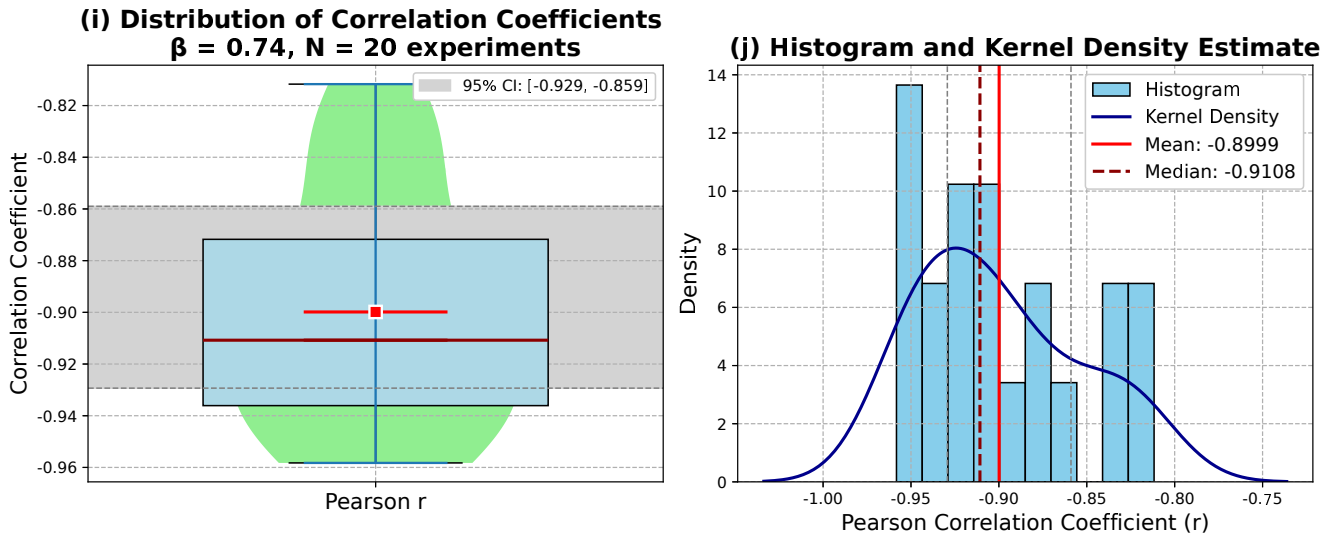


FIG. 3. Statistical distribution of the Pearson correlation coefficients r over repeated experiments. Fig. 3(i) shows a combined box plot and violin plot of the correlation coefficients. The light blue box represents the interquartile range (IQR: -0.9361 to -0.8718), containing the middle 50% of the data. The dark red line inside the box indicates the median value (-0.9108). The light green violin shape illustrates the probability density distribution of the coefficients. The red square marks the mean value (-0.8999). The gray shaded region with dashed boundaries indicates the 95% confidence interval $[-0.9293, -0.8590]$. Fig. 3(j) shows a histogram with kernel density estimation (KDE). The blue bars show the frequency distribution of correlation coefficients. The dark blue curve represents the KDE, providing a smooth estimate of the probability density. The solid red vertical line indicates the mean value (-0.8999), while the dashed gray lines and gray shaded area mark the 95% confidence interval.

periments.

Collectively, these results identify the degradation of quantum resource quality as the underlying mechanism that governs the decline of algorithmic performance. The coherence-to-noise conversion provides a quantitative explanation for optimization stagnation under fixed total resources, offering a mechanistic picture of barren-plateau behavior that goes beyond descriptions based solely on entanglement structure or classical randomness.

Fig. 4 shows the quantum circuit corresponding to the hardware-efficient ansatz described in Sec. V A 4. This circuit prepares the quantum states used to obtain the resource-evolution data in Fig. 2. In the final measurement stage, each qubit is mapped to a distinct classical register, $q_0 \rightarrow c_0$, $q_1 \rightarrow c_1$, $q_2 \rightarrow c_2$, and $q_3 \rightarrow c_3$. This one-to-one mapping facilitates classical post-processing and feedback within the VQA optimization loop. The circuit is designed to ensure

consistent readout for evaluating the resource metrics η , C_{rel} , and \mathcal{D}_{rel} analyzed in Fig. 2.

C. Resource Purity as a Diagnostic Tool

Our results indicate that the BPP arises from a degradation in resource quality. While traditional explanations emphasize entanglement or randomness, our framework highlights the conversion of coherent resources into noise.

The main observations are:

- **Early warning:** A decline in η typically precedes cost-function stagnation, providing an early indicator of BPP.
- **Quality over quantity:** Optimization can fail even when the total amount of resource is approximately

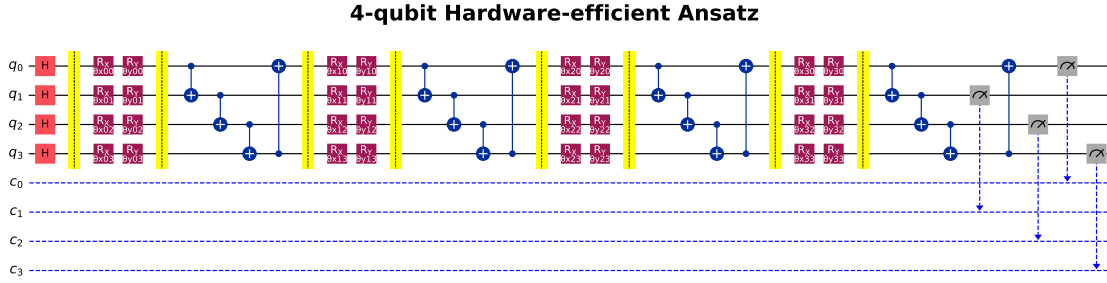


FIG. 4. Circuit diagram of the 4-qubit hardware-efficient ansatz. The circuit consists of an initial Hadamard layer, followed by four parameterized layers of single-qubit rotations and CNOT gates, and a final measurement stage. The measurement outputs are used for classical post-processing and feedback in the VQA loop.

conserved, underscoring that resource quality, not just quantity, is decisive.

- **Mechanism:** The observed anti-correlation between \mathcal{C}_{rel} and \mathcal{D}_{rel} demonstrates the conversion of coherence into noise.

Based on these insights, we propose the following diagnostic protocol:

- Monitor η in real time during the optimization process.
- Adapt the optimization strategy when η drops (for example, by switching optimizers or resetting parameters).
- Use the average value of η to benchmark and compare ansatz architectures, favoring designs that maintain high resource purity.

This resource-based perspective both explains the onset of BPP and informs the design of more robust VQAs. Numerical simulations validate η as a practical and sensitive diagnostic. Tracking resource quality in this way provides a physically transparent route toward noise-resilient algorithms and offers a cross-platform criterion for assessing quantum advantage in current and near-term noisy devices.

VI. CONCLUSION

We have introduced a quantum resource degradation framework that shifts attention from merely quantifying resources to analyzing their internal structure. This framework not only accounts for algorithmic barren plateaus but also offers a unified viewpoint on quantum thermalization, measurement-induced disturbance, and the erosion of quantum advantage in realistic devices.

Our methodology overcomes key shortcomings of standard resource theories by revealing how resources are structurally assembled and how they transform over time. The decomposition of $\mathcal{O}_{\mathcal{C}}$ into \mathcal{C}_{rel} and \mathcal{D}_{rel} enables us to monitor changes in resource quality that conventional scalar resource measures fail to capture.

When applied to VQAs, our theory reframes optimization slowdowns as a degradation of resource quality rather than a simple depletion of resource quantity. The strong negative correlation between \mathcal{C}_{rel} and \mathcal{D}_{rel} , demonstrated in Sec. V B, offers direct evidence for a coherence-to-noise conversion process. This correlation supports the presence of a systematic transformation mechanism at the core of barren plateaus.

The resource purity parameter η functions both as a conceptual lens and as a practical diagnostic tool. It allows early identification of impending optimization stagnation and discriminates between distinct failure mechanisms. Tracking η suggests new avenues for mitigation techniques and for constructing algorithms that are intrinsically more robust to noise.

In a broader sense, this work promotes resource-quality management as an essential counterpart to standard resource quantification. It furnishes a principled framework for understanding and steering optimization behavior on present and near-term noisy quantum platforms.

Future work can be approached at several levels.

On the application side, one may investigate how the η indicator can enable early warnings and adaptive optimization in variational quantum algorithms.

Theoretically, it would be interesting to explore connections between this framework and dynamical signatures such as the Loschmidt echo, and to examine possible extensions to many-body entangled systems.

On the practical side, developing lightweight protocols for estimating η on near-term noisy quantum devices would be a valuable next step.

ACKNOWLEDGMENTS

This research is supported by Jiangxi Province Key Laboratory of Applied Optical Technology [2024SSY03051].

DATA AVAILABILITY

The datasets analysed during the current study are available from the corresponding author on reasonable request.

VII. APPENDIX A: PROOF OF PROPOSITION 1

Proof. 1. **Boundedness:** Since $\mathcal{C}_{\text{rel}}(\rho, \mathcal{C}) \geq 0$ and $\mathcal{D}_{\text{rel}}(\rho) \geq 0$, we have $\mathcal{O}_{\mathcal{C}}(\rho) = \mathcal{C}_{\text{rel}}(\rho, \mathcal{C}) + \mathcal{D}_{\text{rel}}(\rho) \geq \mathcal{C}_{\text{rel}}(\rho, \mathcal{C})$. Therefore, $\eta(\rho) = \mathcal{C}_{\text{rel}}(\rho, \mathcal{C})/\mathcal{O}_{\mathcal{C}}(\rho) \leq 1$. The lower bound $\eta(\rho) \geq 0$ follows directly from the non-negativity of both the numerator and the denominator. By definition, we set $\eta(\rho) = 0$ when $\mathcal{O}_{\mathcal{C}}(\rho) = 0$.

2. **Monotonicity:** For any free operation Λ , the coherence measure \mathcal{C}_{rel} is non-increasing, i.e., $\mathcal{C}_{\text{rel}}(\Lambda(\rho), \mathcal{C}) \leq \mathcal{C}_{\text{rel}}(\rho, \mathcal{C})$. However, the total inconsistency $\mathcal{O}_{\mathcal{C}}$ is not necessarily monotonic under free operations. To analyze η , we consider the changes

$$\begin{aligned}\Delta\mathcal{C}_{\text{rel}} &= \mathcal{C}_{\text{rel}}(\Lambda(\rho)) - \mathcal{C}_{\text{rel}}(\rho) \leq 0, \\ \Delta\mathcal{D}_{\text{rel}} &= \mathcal{D}_{\text{rel}}(\Lambda(\rho)) - \mathcal{D}_{\text{rel}}(\rho), \\ \Delta\mathcal{O}_{\mathcal{C}} &= \Delta\mathcal{C}_{\text{rel}} + \Delta\mathcal{D}_{\text{rel}}.\end{aligned}\quad (28)$$

Then

$$\eta(\Lambda(\rho)) - \eta(\rho) = \frac{\mathcal{C}_{\text{rel}}(\rho) + \Delta\mathcal{C}_{\text{rel}}}{\mathcal{O}_{\mathcal{C}}(\rho) + \Delta\mathcal{O}_{\mathcal{C}}} - \frac{\mathcal{C}_{\text{rel}}(\rho)}{\mathcal{O}_{\mathcal{C}}(\rho)}. \quad (29)$$

The denominator is positive, so the sign of the difference is determined by the numerator after cross-multiplication:

$$\begin{aligned}(\mathcal{C}_{\text{rel}}(\rho) + \Delta\mathcal{C}_{\text{rel}}) \mathcal{O}_{\mathcal{C}}(\rho) - \mathcal{C}_{\text{rel}}(\rho) (\mathcal{O}_{\mathcal{C}}(\rho) + \Delta\mathcal{O}_{\mathcal{C}}) \\ = \Delta\mathcal{C}_{\text{rel}} \mathcal{O}_{\mathcal{C}}(\rho) - \mathcal{C}_{\text{rel}}(\rho) \Delta\mathcal{O}_{\mathcal{C}}.\end{aligned}\quad (30)$$

Since $\Delta\mathcal{C}_{\text{rel}} \leq 0$ and $\mathcal{O}_{\mathcal{C}}(\rho) \geq \mathcal{C}_{\text{rel}}(\rho)$, if $\Delta\mathcal{O}_{\mathcal{C}} \geq 0$ the above expression is ≤ 0 . If $\Delta\mathcal{O}_{\mathcal{C}} < 0$, further analysis is required. Free operations may reduce the total inconsistency, but they cannot convert noise into coherence. Using the data-processing inequality for \mathcal{C}_{rel} together with the decomposition structure of OE, one finds that a free operation cannot increase η . Suppose, for contradiction, that there exists a free operation Λ such that $\eta(\Lambda(\rho)) > \eta(\rho)$. This would imply that the relative decrease in \mathcal{C}_{rel} is smaller than the relative decrease in $\mathcal{O}_{\mathcal{C}}$, effectively meaning that noise is converted into coherence. This contradicts the fact that free operations cannot create coherence. Therefore, $\eta(\Lambda(\rho)) \leq \eta(\rho)$ for any free operation Λ .

3. **Strict decrease under degradation channels:** For the degradation channel $\Lambda_{\alpha, \beta}$, with probability α the channel replaces the state by a block-diagonal state (either dephased or projected). This strictly reduces the coherence \mathcal{C}_{rel} unless the initial state is already incoherent. By Theorem 1, such channels approximately conserve $\mathcal{O}_{\mathcal{C}}$ for suitable parameters. Thus, the numerator strictly decreases while the denominator remains approximately constant, leading to a strict decrease in η . \square

VIII. APPENDIX B: PROOF OF THEOREM 1

Proof. Step 1: System and coarse-graining setup

Consider a four-dimensional quantum system with Hilbert space $\mathcal{H} = \mathbb{C}^4$ and computational basis $\{|00\rangle, |01\rangle, |10\rangle, |11\rangle\}$. We introduce the coarse-graining $\mathcal{C} = \{\hat{P}_1, \hat{P}_2\}$ with

$$\begin{aligned}\hat{P}_1 &= |00\rangle\langle 00| + |01\rangle\langle 01|, \\ \hat{P}_2 &= |10\rangle\langle 10| + |11\rangle\langle 11|,\end{aligned}\quad (31)$$

so that the corresponding subspaces have volumes $V_1 = V_2 = 2$ and maximally mixed reference states

$$\kappa_1 = \frac{1}{2}|00\rangle\langle 00| + \frac{1}{2}|01\rangle\langle 01|, \quad (32)$$

$$\kappa_2 = \frac{1}{2}|10\rangle\langle 10| + \frac{1}{2}|11\rangle\langle 11|. \quad (33)$$

Step 2: Initial state

We now specify an initial state ρ that makes the resource-degradation mechanism transparent:

$$\begin{aligned}\rho = \frac{3}{8}|00\rangle\langle 00| + \frac{1}{4}|00\rangle\langle 11| + \frac{1}{8}|01\rangle\langle 01| \\ + \frac{1}{8}|10\rangle\langle 10| + \frac{1}{4}|11\rangle\langle 00| + \frac{3}{8}|11\rangle\langle 11|.\end{aligned}\quad (34)$$

This state has the following properties:

- It carries **nontrivial coarse-grained coherence** \mathcal{C}_{rel} between the subspaces \mathcal{H}_1 and \mathcal{H}_2 , as signaled by the off-diagonal terms $|00\rangle\langle 11|$ and $|11\rangle\langle 00|$.
- It has **nontrivial intra-block structure** within each coarse-grained subspace, so that changes in purity under the dynamics can be tracked explicitly.
- Its eigenvalues $\lambda_1 = \frac{5}{8}$ and $\lambda_2 = \lambda_3 = \lambda_4 = \frac{1}{8}$ show that ρ is mixed but not maximally mixed, leaving room for coherence to be converted into classical noise.
- It thus captures a generic physical situation in which a quantum system starts with substantial coherence resources across a coarse-graining, which can subsequently be degraded by noisy operations.

This choice strikes a balance between physical relevance and analytical tractability, and it allows us to clearly exhibit how coarse-grained coherence is irreversibly converted into local noise under the dynamics considered below.

Step 3: Calculation of Initial Resource Metrics

(a) $\mathcal{C}_{\text{rel}}(\rho, \mathcal{C})$

We first compute the block-diagonal state obtained after dephasing:

$$\begin{aligned}\hat{P}_1\rho\hat{P}_1 &= \frac{3}{8}|00\rangle\langle 00| + \frac{1}{8}|01\rangle\langle 01|, \\ \hat{P}_2\rho\hat{P}_2 &= \frac{1}{8}|10\rangle\langle 10| + \frac{3}{8}|11\rangle\langle 11|.\end{aligned}\quad (35)$$

Using the definition

$$\mathcal{C}_{\text{rel}}(\rho, \mathcal{C}) = S(\Delta(\rho)) - S(\rho), \quad (36)$$

we have

$$\begin{aligned}\Delta(\rho) &= \hat{P}_1 \rho \hat{P}_1 + \hat{P}_2 \rho \hat{P}_2 \\ &= \frac{3}{8} |00\rangle\langle 00| + \frac{1}{8} |01\rangle\langle 01| + \frac{1}{8} |10\rangle\langle 10| \\ &\quad + \frac{3}{8} |11\rangle\langle 11|,\end{aligned}\quad (37)$$

so that

$$\begin{aligned}S(\rho) &= -\frac{5}{8} \log_2 \frac{5}{8} - \frac{3}{8} \log_2 \frac{3}{8}, \\ S(\Delta(\rho)) &= -\frac{3}{4} \log_2 \frac{3}{8} - \frac{1}{4} \log_2 \frac{1}{8}.\end{aligned}\quad (38)$$

Therefore,

$$\mathcal{C}_{\text{rel}}(\rho, \mathcal{C}) = -\frac{3}{4} \log_2 \frac{3}{8} + \frac{5}{8} \log_2 \frac{5}{8} + \frac{1}{8} \log_2 \frac{1}{8}. \quad (39)$$

(b) Intra-block Noise $\mathcal{D}_{\text{rel}}(\rho)$

We next compute the conditional states within each subspace and their deviation from the maximally mixed state:

$$\begin{aligned}\rho_1 &= \frac{\hat{P}_1 \rho \hat{P}_1}{p_1} = \frac{3}{4} |00\rangle\langle 00| + \frac{1}{4} |01\rangle\langle 01|, \\ \rho_2 &= \frac{\hat{P}_2 \rho \hat{P}_2}{p_2} = \frac{1}{4} |10\rangle\langle 10| + \frac{3}{4} |11\rangle\langle 11|.\end{aligned}\quad (40)$$

The corresponding relative entropies are

$$\begin{aligned}D[\rho_1 \|\kappa_1] &= \text{Tr}[\rho_1 (\log_2 \rho_1 - \log_2 \kappa_1)] \\ &= \frac{3}{4} \log_2 3 - 1, \\ D[\rho_2 \|\kappa_2] &= \text{Tr}[\rho_2 (\log_2 \rho_2 - \log_2 \kappa_2)] \\ &= \frac{3}{4} \log_2 3 - 1.\end{aligned}\quad (41)$$

For $p_1 = p_2 = 1/2$ we obtain

$$\mathcal{D}_{\text{rel}}(\rho) = \sum_x p_x D[\rho_x \|\kappa_x] = \frac{3}{4} \log_2 3 - 1. \quad (42)$$

(c) Total Inconsistency

$$\begin{aligned}\mathcal{O}_{\mathcal{C}}(\rho) &= \mathcal{C}_{\text{rel}}(\rho, \mathcal{C}) + \mathcal{D}_{\text{rel}}(\rho) \\ &= -\frac{3}{4} \log_2 \frac{3}{8} + \frac{5}{8} \log_2 \frac{5}{8} \\ &\quad + \frac{1}{8} \log_2 \frac{1}{8} + \frac{3}{4} \log_2 3 - 1.\end{aligned}\quad (43)$$

Step 4: Construction of the Degradation Channel

We define the free operation as

$$\Lambda_{\varepsilon}(\rho) = (1 - \varepsilon)\rho + \varepsilon |00\rangle\langle 00|, \quad (44)$$

where $0 \leq \varepsilon \leq 1$.

- **Why is this a free operation?** This channel probabilistically replaces the state with the fixed block-incoherent state $|00\rangle\langle 00|$. In the resource theory of block coherence, operations that prepare or introduce BI states are taken to be free, since they cannot generate \mathcal{C}_{rel} . The map Λ_{ε} is a convex combination of such preparation maps and is therefore free.

- **Why do we choose this operation?** This channel is minimal in structure, yet making the degradation mechanism transparent. With probability ε , the system is reset to a pure state that is block-diagonal under the chosen coarse-graining, which directly suppresses coherence between different blocks ($\Delta\mathcal{C}_{\text{rel}} < 0$). At the same time, because the reset state is pure, it has maximal purity within its block and thus increases the intra-block order \mathcal{D}_{rel} ($\Delta\mathcal{D}_{\text{rel}} > 0$). By tuning ε , we can continuously control the degree of degradation and verify that $\Delta\mathcal{O}_{\mathcal{C}} \approx 0$ for suitable parameters.

After this operation acts on the initial state ρ , we obtain

$$\begin{aligned}\Lambda_{\varepsilon}(\rho) &= \frac{3+5\varepsilon}{8} |00\rangle\langle 00| + \frac{1-\varepsilon}{4} |00\rangle\langle 11| \\ &\quad + \frac{1-\varepsilon}{8} |01\rangle\langle 01| + \frac{1-\varepsilon}{8} |10\rangle\langle 10| \\ &\quad + \frac{1-\varepsilon}{4} |11\rangle\langle 00| + \frac{3-3\varepsilon}{8} |11\rangle\langle 11|,\end{aligned}\quad (45)$$

with eigenvalues

$$\lambda_1^{\varepsilon} = \lambda_2^{\varepsilon} = \frac{1-\varepsilon}{8}, \quad (46)$$

$$\lambda_3^{\varepsilon} = \frac{3+\varepsilon-2\sqrt{5\varepsilon^2-2\varepsilon+1}}{8}, \quad (47)$$

$$\lambda_4^{\varepsilon} = \frac{3+\varepsilon+2\sqrt{5\varepsilon^2-2\varepsilon+1}}{8}. \quad (48)$$

Step 5: Final Resource Quantities

(a) $\mathcal{C}_{\text{rel}}(\Lambda_{\varepsilon}(\rho), \mathcal{C})$

We first project onto the blocks:

$$\begin{aligned}\hat{P}_1 \Lambda_{\varepsilon}(\rho) \hat{P}_1 &= \frac{3+5\varepsilon}{8} |00\rangle\langle 00| + \frac{1-\varepsilon}{8} |01\rangle\langle 01|, \\ \hat{P}_2 \Lambda_{\varepsilon}(\rho) \hat{P}_2 &= \frac{1-\varepsilon}{8} |10\rangle\langle 10| + \frac{3-3\varepsilon}{8} |11\rangle\langle 11|.\end{aligned}\quad (49)$$

Using the definition

$$\mathcal{C}_{\text{rel}}(\Lambda_{\varepsilon}(\rho), \mathcal{C}) = S(\Delta[\Lambda_{\varepsilon}(\rho)]) - S(\Lambda_{\varepsilon}(\rho)), \quad (50)$$

we note that

$$\begin{aligned}\Delta(\Lambda_{\varepsilon}(\rho)) &= \hat{P}_1 \Lambda_{\varepsilon}(\rho) \hat{P}_1 + \hat{P}_2 \Lambda_{\varepsilon}(\rho) \hat{P}_2 \\ &= \frac{3+5\varepsilon}{8} |00\rangle\langle 00| + \frac{1-\varepsilon}{8} |01\rangle\langle 01| \\ &\quad + \frac{1-\varepsilon}{8} |10\rangle\langle 10| + \frac{3-3\varepsilon}{8} |11\rangle\langle 11|.\end{aligned}\quad (51)$$

Thus

$$\begin{aligned}S(\Lambda_{\varepsilon}(\rho)) &= -\frac{1-\varepsilon}{4} \log_2 \frac{1-\varepsilon}{8} \\ &\quad - \lambda_3^{\varepsilon} \log_2 \lambda_3^{\varepsilon} - \lambda_4^{\varepsilon} \log_2 \lambda_4^{\varepsilon},\end{aligned}\quad (52)$$

$$\begin{aligned} S(\Delta(\Lambda_\varepsilon(\rho))) &= -\frac{3+5\varepsilon}{8} \log_2 \frac{3+5\varepsilon}{8} \\ &\quad -\frac{1-\varepsilon}{4} \log_2 \frac{1-\varepsilon}{8} \\ &\quad -\frac{3-3\varepsilon}{8} \log_2 \frac{3-3\varepsilon}{8}. \end{aligned} \quad (53)$$

Therefore,

$$\begin{aligned} \mathcal{C}_{\text{rel}}(\Lambda_\varepsilon(\rho), \mathcal{C}) &= -\frac{3-3\varepsilon}{8} \log_2 \frac{3-3\varepsilon}{8} \\ &\quad -\frac{3+5\varepsilon}{8} \log_2 \frac{3+5\varepsilon}{8} \\ &\quad +\lambda_3^\varepsilon \log_2 \lambda_3^\varepsilon + \lambda_4^\varepsilon \log_2 \lambda_4^\varepsilon. \end{aligned} \quad (54)$$

(b) Intra-block noise $\sum_x p_x^\varepsilon D[\rho_x^\varepsilon \|\kappa_x]$

For $p_1^\varepsilon = \frac{1+\varepsilon}{2}$ and $p_2^\varepsilon = \frac{1-\varepsilon}{2}$, we obtain

$$\begin{aligned} \rho_1^\varepsilon &= \frac{\hat{P}_1 \Lambda_\varepsilon(\rho) \hat{P}_1}{p_1^\varepsilon} = \frac{3+5\varepsilon}{4(1+\varepsilon)} |00\rangle\langle 00| \\ &\quad + \frac{1-\varepsilon}{4(1+\varepsilon)} |01\rangle\langle 01|, \end{aligned} \quad (55)$$

$$\rho_2^\varepsilon = \frac{\hat{P}_2 \Lambda_\varepsilon(\rho) \hat{P}_2}{p_2^\varepsilon} = \frac{1}{4} |10\rangle\langle 10| + \frac{3}{4} |11\rangle\langle 11|. \quad (56)$$

The corresponding quantum relative entropies are

$$\begin{aligned} D[\rho_1^\varepsilon \|\kappa_1] &= \text{Tr}[\rho_1^\varepsilon (\log_2 \rho_1^\varepsilon - \log_2 \kappa_1)] \\ &= \frac{3+5\varepsilon}{4(1+\varepsilon)} \log_2 \frac{3+5\varepsilon}{4(1+\varepsilon)} \\ &\quad + \frac{1-\varepsilon}{4(1+\varepsilon)} \log_2 \frac{1-\varepsilon}{4(1+\varepsilon)} + 1, \end{aligned} \quad (57)$$

$$D[\rho_2^\varepsilon \|\kappa_2] = \frac{3}{4} \log_2 3 - 1,$$

and hence

$$\begin{aligned} \mathcal{D}_{\text{rel}}(\Lambda_\varepsilon(\rho)) &= \frac{3+5\varepsilon}{8} \log_2 \frac{3+5\varepsilon}{4(1+\varepsilon)} \\ &\quad + \frac{1-\varepsilon}{8} \log_2 \frac{27(1-\varepsilon)}{4(1+\varepsilon)} + \varepsilon. \end{aligned} \quad (58)$$

- [1] J. Åberg, Quantifying superposition (2006), [arXiv:quant-ph/0612146 \[quant-ph\]](https://arxiv.org/abs/quant-ph/0612146).
- [2] T. Baumgratz, M. Cramer, and M. B. Plenio, Quantifying coherence, *Phys. Rev. Lett.* **113**, 140401 (2014).
- [3] F. Bischof, H. Kampermann, and D. Bruß, Resource theory of coherence based on positive-operator-valued measures, *Phys. Rev. Lett.* **123**, 110402 (2019).
- [4] J. Xu, L.-H. Shao, and S.-M. Fei, Coherence measures with respect to general quantum measurements, *Phys. Rev. A* **102**, 012411 (2020).
- [5] S. Kim, C. Xiong, A. Kumar, G. Zhang, and J. Wu,

(c) Total inconsistency $\mathcal{O}_{\mathcal{C}}(\Lambda_\varepsilon(\rho))$

Finally,

$$\begin{aligned} \mathcal{O}_{\mathcal{C}}(\Lambda_\varepsilon(\rho)) &= \mathcal{C}_{\text{rel}}(\Lambda_\varepsilon(\rho), \mathcal{C}) + \mathcal{D}_{\text{rel}}(\Lambda_\varepsilon(\rho)) \\ &= \lambda_3^\varepsilon \log_2 \lambda_3^\varepsilon - \frac{3+5\varepsilon}{8} \log_2 \frac{1+\varepsilon}{2} \\ &\quad - \frac{3-3\varepsilon}{8} \log_2 \frac{1-\varepsilon}{8} + \lambda_4^\varepsilon \log_2 \lambda_4^\varepsilon \\ &\quad + \frac{1-\varepsilon}{8} \log_2 \frac{1-\varepsilon}{4(1+\varepsilon)} + \varepsilon. \end{aligned} \quad (59)$$

For $\varepsilon = 0.26$, we obtain the following results:

$$\begin{aligned} \Delta\mathcal{C}_{\text{rel}} &= \mathcal{C}_{\text{rel}}(\Lambda_\varepsilon(\rho), \mathcal{C}) - \mathcal{C}_{\text{rel}}(\rho, \mathcal{C}) \approx -0.12986, \\ \Delta\mathcal{D}_{\text{rel}} &= \mathcal{D}_{\text{rel}}(\Lambda_\varepsilon(\rho)) - \mathcal{D}_{\text{rel}}(\rho) \approx 0.12898, \\ \Delta\mathcal{O}_{\mathcal{C}} &= \mathcal{O}_{\mathcal{C}}(\Lambda_\varepsilon(\rho)) - \mathcal{O}_{\mathcal{C}}(\rho) \approx -0.00089, \end{aligned} \quad (60)$$

and

$$\begin{aligned} \eta(\rho) &\approx 0.58174, \quad \eta(\Lambda_\varepsilon(\rho)) \approx 0.29450, \\ \mathcal{O}_{\mathcal{C}}(\rho) &\approx 0.45121, \quad \frac{|\Delta\mathcal{C}_{\text{rel}}|}{\mathcal{O}_{\mathcal{C}}(\rho)} \approx 0.28735. \end{aligned} \quad (61)$$

These results satisfy the following conditions:

$$\begin{aligned} \Delta\mathcal{C}_{\text{rel}} &< 0, \quad \Delta\mathcal{D}_{\text{rel}} > 0, \quad |\Delta\mathcal{D}_{\text{rel}}| \approx |\Delta\mathcal{C}_{\text{rel}}|, \\ \Delta\mathcal{O}_{\mathcal{C}} &\approx 0, \quad \eta(\Lambda_\varepsilon(\rho)) \approx \eta(\rho) - \frac{|\Delta\mathcal{C}_{\text{rel}}|}{\mathcal{O}_{\mathcal{C}}(\rho)}. \end{aligned} \quad (62)$$

□

We find $\Delta\eta \approx 0.28724$, which signals a marked deterioration in the quality of the quantum resource, i.e., a significant degradation of the resource under the free operation Λ_ε . In contrast, $\Delta\mathcal{O}_{\mathcal{C}} \approx 0$ indicates that the overall amount of resource is essentially conserved. These results are in complete agreement with our theoretical predictions and illustrate how a free operation can severely impair resource quality while leaving the total resource content nearly unchanged, a mechanism that is expected to be generic across different quantum resource theories and therefore broadly relevant for quantum many-body and information-processing scenarios.

- Quantifying dynamical coherence with coherence measures, *Phys. Rev. A* **104**, 012404 (2021).
- [6] A. E. Rastegin, Quantum-coherence quantifiers based on the tsallis relative α entropies, *Phys. Rev. A* **93**, 032136 (2016).
- [7] D. Šafránek, J. M. Deutsch, and A. Aguirre, Quantum coarse-grained entropy and thermodynamics, *Phys. Rev. A* **99**, 010101 (2019).
- [8] D. Šafránek, J. M. Deutsch, and A. Aguirre, Quantum coarse-grained entropy and thermalization in closed systems, *Phys. Rev. A* **99**, 012103 (2019).
- [9] D. Šafránek, A. Aguirre, S. Joseph, and J. M.

Deutsch, A brief introduction to observational entropy, *Foundations of Physics* **51**, 101 (2021).

[10] J. Schindler, D. Šafránek, and A. Aguirre, Quantum correlation entropy, *Phys. Rev. A* **102**, 052407 (2020).

[11] P. Strasberg and A. Winter, First and second law of quantum thermodynamics: A consistent derivation based on a microscopic definition of entropy, *PRX Quantum* **2**, 030202 (2021).

[12] Z. Xiang, Superposition measures with respect to coarse-grained measurement in the generalized n-qubit werner state, *Quantum Inf. Process.* **22**, 156 (2023).

[13] F. Buscemi, J. Schindler, and D. Šafránek, Observational entropy, coarse-grained states, and the petz recovery map: information-theoretic properties and bounds, *New Journal of Physics* **25**, 053002 (2023), [arXiv:2209.03803 \[quant-ph\]](https://arxiv.org/abs/2209.03803).

[14] G. Bai, D. Šafránek, J. Schindler, F. Buscemi, and V. Scarani, Observational entropy with general quantum priors, *Quantum* **8**, 1524 (2024).

[15] J. R. McClean, S. Boixo, V. N. Smelyanskiy, R. Babbush, and H. Neven, Barren plateaus in quantum neural network training landscapes, *Nat. Commun.* **9**, 4812 (2018).

[16] M. Cerezo, A. Arrasmith, R. Babbush, S. C. Benjamin, S. Endo, K. Fujii, J. R. McClean, K. Mitarai, X. Yuan, L. Cincio, and P. J. Coles, Variational quantum algorithms, *Nat. Rev. Phys.* **3**, 625 (2021).

[17] I. Marvian and R. W. Spekkens, The theory of manipulations of pure state asymmetry: I. basic tools, equivalence classes and single copy transformations, *New Journal of Physics* **15**, 033001 (2013).

[18] I. Marvian and R. W. Spekkens, Extending noether's theorem by quantifying the asymmetry of quantum states, *Nat. Commun.* **5**, 3821 (2014).

[19] G. Gour, I. Marvian, and R. W. Spekkens, Measuring the quality of a quantum reference frame: The relative entropy of frame-ness, *Phys. Rev. A* **80**, 012307 (2009).

[20] I. Marvian, R. W. Spekkens, and P. Zanardi, Quantum speed limits, coherence, and asymmetry, *Phys. Rev. A* **93**, 052331 (2016).

[21] I. Marvian and R. W. Spekkens, How to quantify coherence: Distinguishing speakable and unspeakable notions, *Phys. Rev. A* **94**, 052324 (2016).

[22] S. Sachdev, *Quantum Phase Transitions*, 2nd ed. (Cambridge University Press, 2011).

[23] Z. Holmes, K. Sharma, M. Cerezo, and P. J. Coles, Connecting ansatz expressibility to gradient magnitudes and barren plateaus, *PRX Quantum* **3**, 010313 (2022).

[24] S. Wang, E. Fontana, M. Cerezo, K. Sharma, A. Sone, L. Cincio, and P. J. Coles, Noise-induced barren plateaus in variational quantum algorithms, *Nature Communications* **12**, 6961 (2021).